Quarkonium measurements with ATHENA through dielectrons and dimuons

Short overview

Leszek Kosarzewski

Faculty of Nuclear Sciences and Physical Engineering
Czech Technical University in Prague

EIC Quarkonium 25.4.2022

EUROPEAN UNION
European Structural and Investment Funds
Operational Programme Research,
Development and Education

MINISTRY OF EDUCATION,
YOUTH AND SPORTS

ČVUT
ČESKÉ VYSOKÉ
UČENÍ TECHNICKÉ
V PRAZE

FJFI

Outline

Introduction

- This is a very quick overview (very limited time to prepare)
- Based on ATHENA proposal and responses to DPAP questions
  - Used information from the proposal submitted here: [https://indico.bnl.gov/event/13614/]
- Intended as a reference for the discussion

ATHENA detector overview

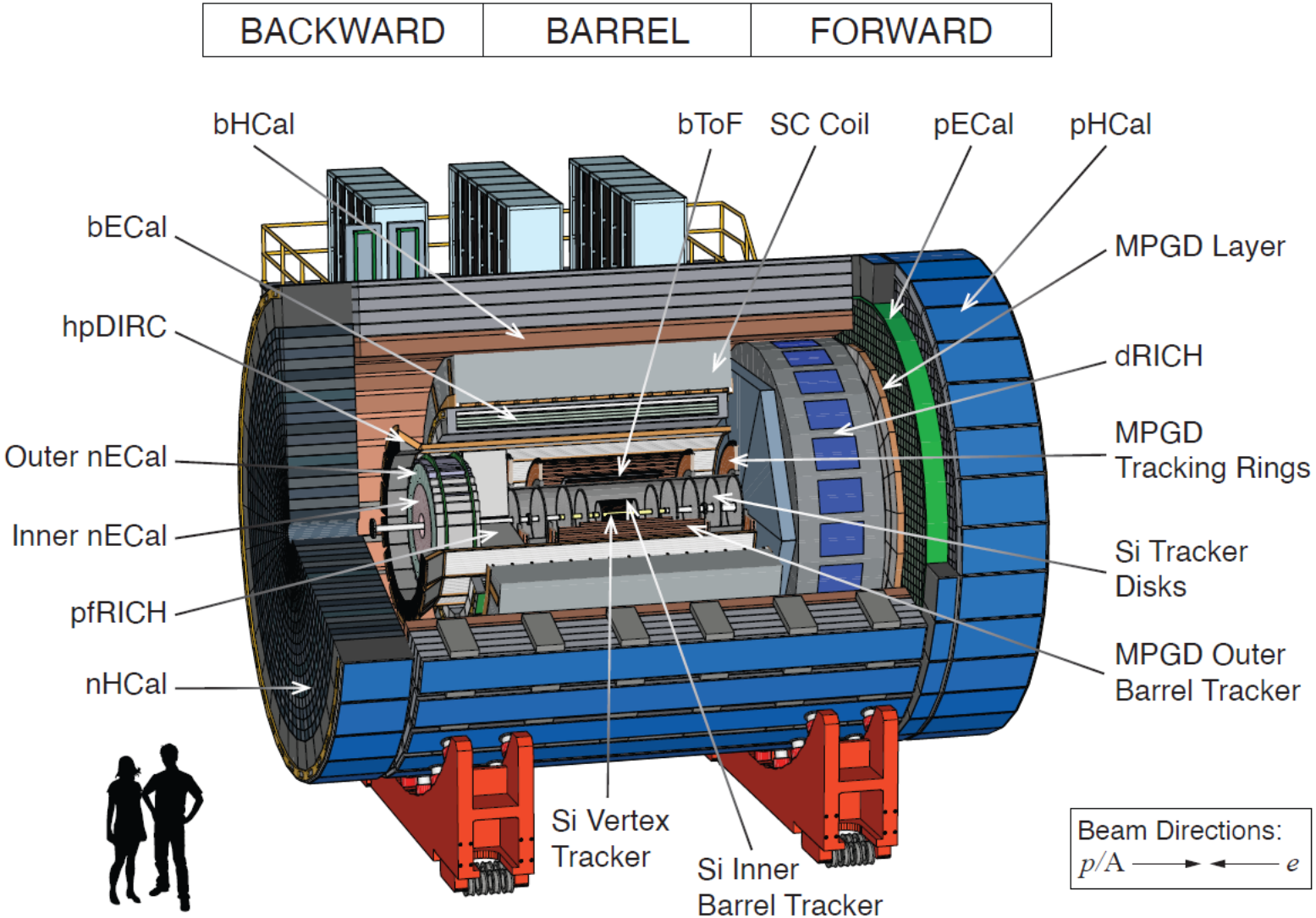

Table 1.1: Complete list of ATHENA subsystems in the main detector ordered from small to large radii (barrel) and increasing distance from the interaction point (forward and backward regions). The PID range in momentum is quoted for 3σ separation.

	Detector	Purpose	Technology	Acceptance	PID Range (GeV/c)
Forward (h-going)	Si-Tracker Disks	Tracking	6 disks of MAPS	$1.1 < \eta < 3.75$	
	Tracking Rings (MPGD)	Tracking	Planar GEMs with annular shape surrounding the Si-disks	$1.1 < \eta < 2.0$	
	dRICH	PID	Dual RICH with aerogel and gas	$1.2 < \eta < 3.7$	$3 < p < 60$ (K/π) $0.85 < p < 15$ (e/π)
	MPGD Layer	Tracking	Planar μRWell disk	$1.4 < \eta < 3.75$	
	pECal	e/m Calorimetry	W-Powder/SciFi calorimeter	$1.2 < \eta < 4.0$	
	pHCal	Hadron Calorimetry	Fe/Sci sandwich	$1 < \eta < 4.0$	
Barrel	Si Vertex-Tracker	Tracking and Vertexing	3-layer MAPS	$-2.2 < \eta < 2.2$	
	Si Barrel-Tracker	Tracking	2-layer MAPS	$-1.05 < \eta < 1.05$	
	bToF	PID and Tracking	AC-LGAD	$-1.05 < \eta < 1.05$ $p_T > 0.23$ GeV/c @ 3T	$p < 1.3$ (K/π) $p < 0.4$ (e/π)
	Barrel Tracker (MPGD)	Tracking	4 (2+2) layer cylindrical Micromegas	$-1.05 < \eta < 1.05$	
	hpDIRC	PID	DIRC with focusing elements and fine pixel readout	$-1.64 < \eta < 1.25$ $p_T > 0.45$ GeV/c @ 3T	$p < 6.5$ (K/π) $p < 1.2$ (e/π)
	bECal	e/m Calorimetry & Tracking	Hybrid with Astropix imaging layers alternated with Pb/SciFi layers followed by a set of Pb/SciFi layers	$-1.5 < \eta < 1.2$	
	bHCal	Hadron Calorimetry	Fe/Sci sandwich	$-1.0 < \eta < 1.0$	
Backward (e-going)	Si-Tracker Disks	Tracking	5 disks of MAPS	$-1.1 > \eta > -3.8$	
	Tracking Rings (MPGD)	Tracking	Planar GEMs with annular shape surrounding the Si-disks	$-1.1 > \eta > -1.8$	
	pfRICH	PID	Proximity focusing RICH with aerogel	$-1.5 > \eta > -3.8$	$3 < p < 11$ (K/π) $0.85 < p < 3$ (e/π)
	Inner nECal	e/m Calorimetry	$PbWO_4$	$-2.3 > \eta > -4.0$	
	Outer nECal	e/m Calorimetry	SciGlass	$-1.5 > \eta > -2.3$	
	nHCal	Hadron Calorimetry	Fe/Sci sandwich	$-1 > \eta > -4$	

Tracker

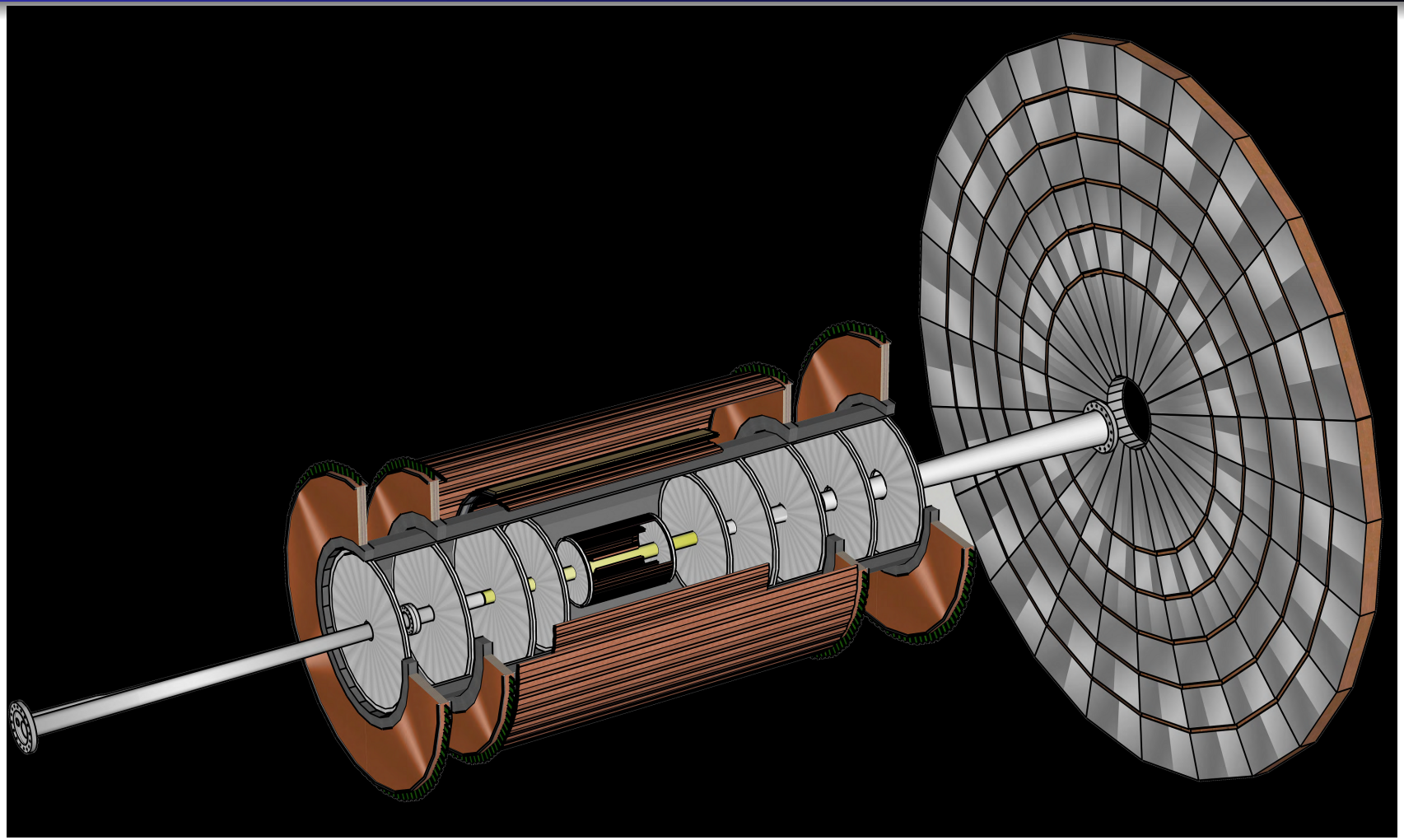

- Silicon sensors:
  - 3 vertex and 2 barrel layers
  - MAPS sensors similar to ALICE ITS3 upgrade
- 4 Micromegas barrel trackers
- GEM disks: 5 *e*-going (backward) and 6 *p*-going (forward)
- Large forward μRWell detector

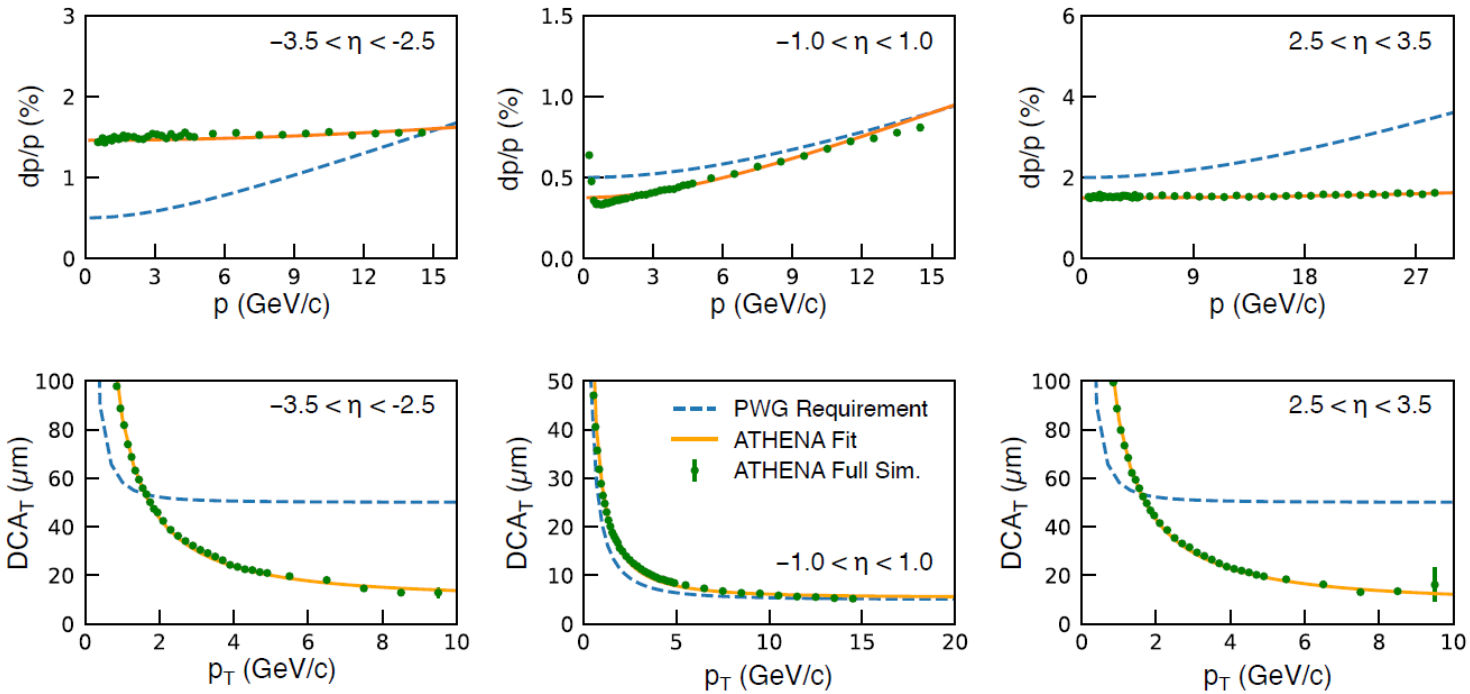

Figure 2.4: ATHENA tracking performance of generated pions compared to the Yellow Report requirements (dashed lines) for selected η bins. Top row: momentum resolutions versus momentum. Bottom row: Transverse DCA performance versus momentum (FullSim).

Tracker performance vs. requirements

Table 2.2: Comparison of performance and Yellow Report requirement parameterizations for relative momentum and transverse pointing resolutions as a function of momentum for the ATHENA baseline tracking system.

	Momentum resolution $\sigma(p)/p$		**Transverse pointing resolution** $\sigma(\mathrm{DCA_T})$	
	Performance	Requirements	Performance	Requirements
$-3.5 < \eta < -2.5$	$\sim 0.04\% \times p \oplus 1.5\%$	$\sim 0.1\% \times p \oplus 0.5\%$	$\sim 80/p_T \oplus 10\ \mu m$	$\sim 30/p_T \oplus 50\ \mu m$
$-2.5 < \eta < -1.0$	$\sim 0.01\% \times p \oplus 0.5\%$	$\sim 0.05\% \times p \oplus 0.5\%$	$\sim 50/p_T \oplus 5\ \mu m$	$\sim 30/p_T \oplus 20\ \mu m$
$-1.0 < \eta < 1.0$	$\sim 0.05\% \times p \oplus 0.4\%$	$\sim 0.05\% \times p \oplus 0.5\%$	$\sim 30/p_T \oplus 5\ \mu m$	$\sim 20/p_T \oplus 5\ \mu m$
$1.0 < \eta < 2.5$	$\sim 0.01\% \times p \oplus 0.5\%$	$\sim 0.05\% \times p \oplus 1\%$	$\sim 50/p_T \oplus 5\ \mu m$	$\sim 30/p_T \oplus 20\ \mu m$
$2.5 < \eta < 3.5$	$\sim 0.02\% \times p \oplus 1.5\%$	$\sim 0.1\% \times p \oplus 2\%$	$\sim 80/p_T \oplus 10\ \mu m$	$\sim 30/p_T \oplus 50\ \mu m$

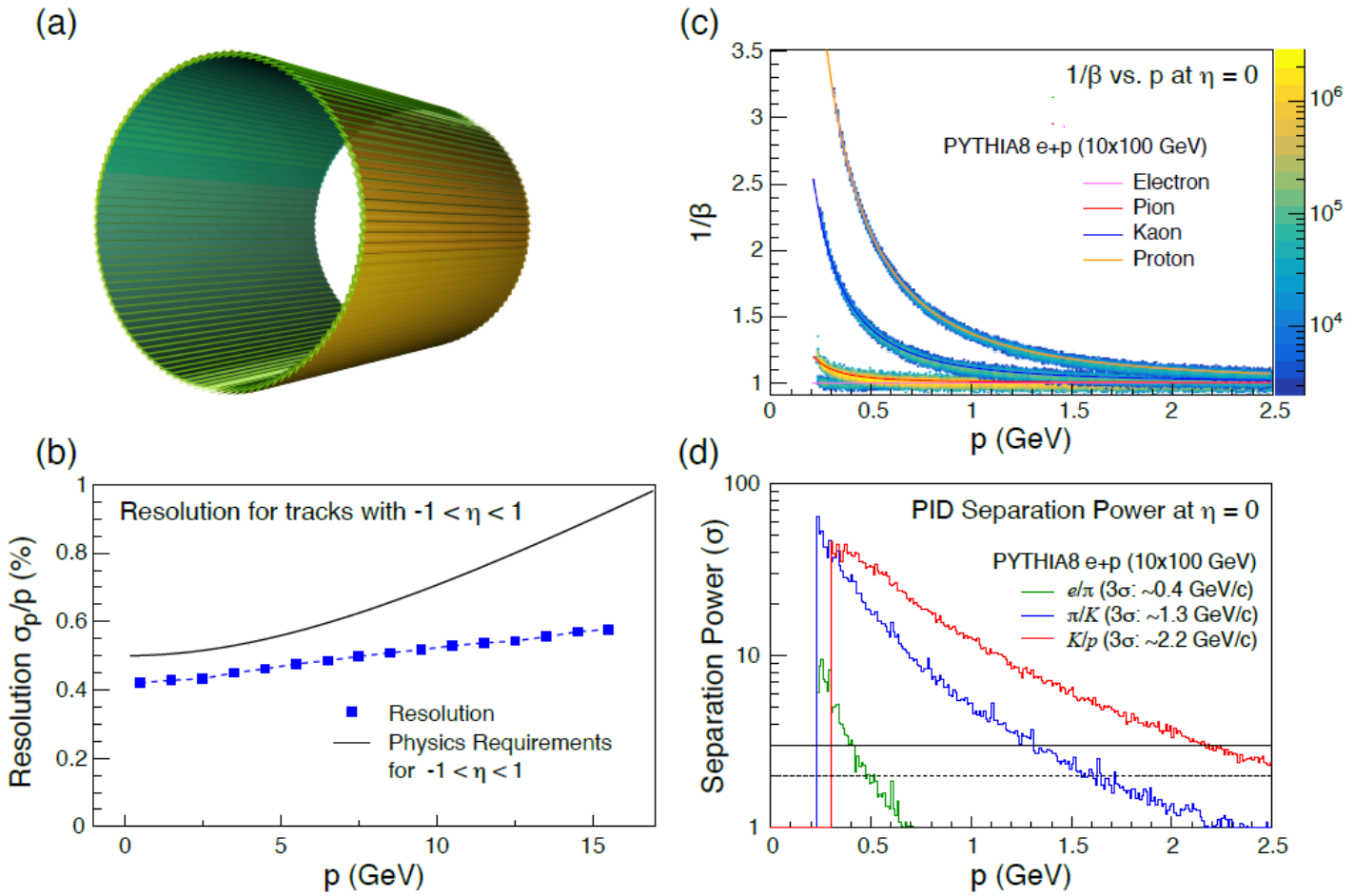

Figure 2.10: a) Configuration of the barrel ToF. b) Anticipated impact from the spatial hit from the ToF system on the tracking performance, with improved baseline performance at higher momenta. c) Shows that ToF more than satisfies the PID requirements in the momentum range below the DIRC kaon threshold (0.47 GeV/c), thereby filling in the PID to 230 MeV/c. d) Separation power in number of σ separation (FullSim).

- AC-coupled LGAD (low-gain avalanche diodes) TOF

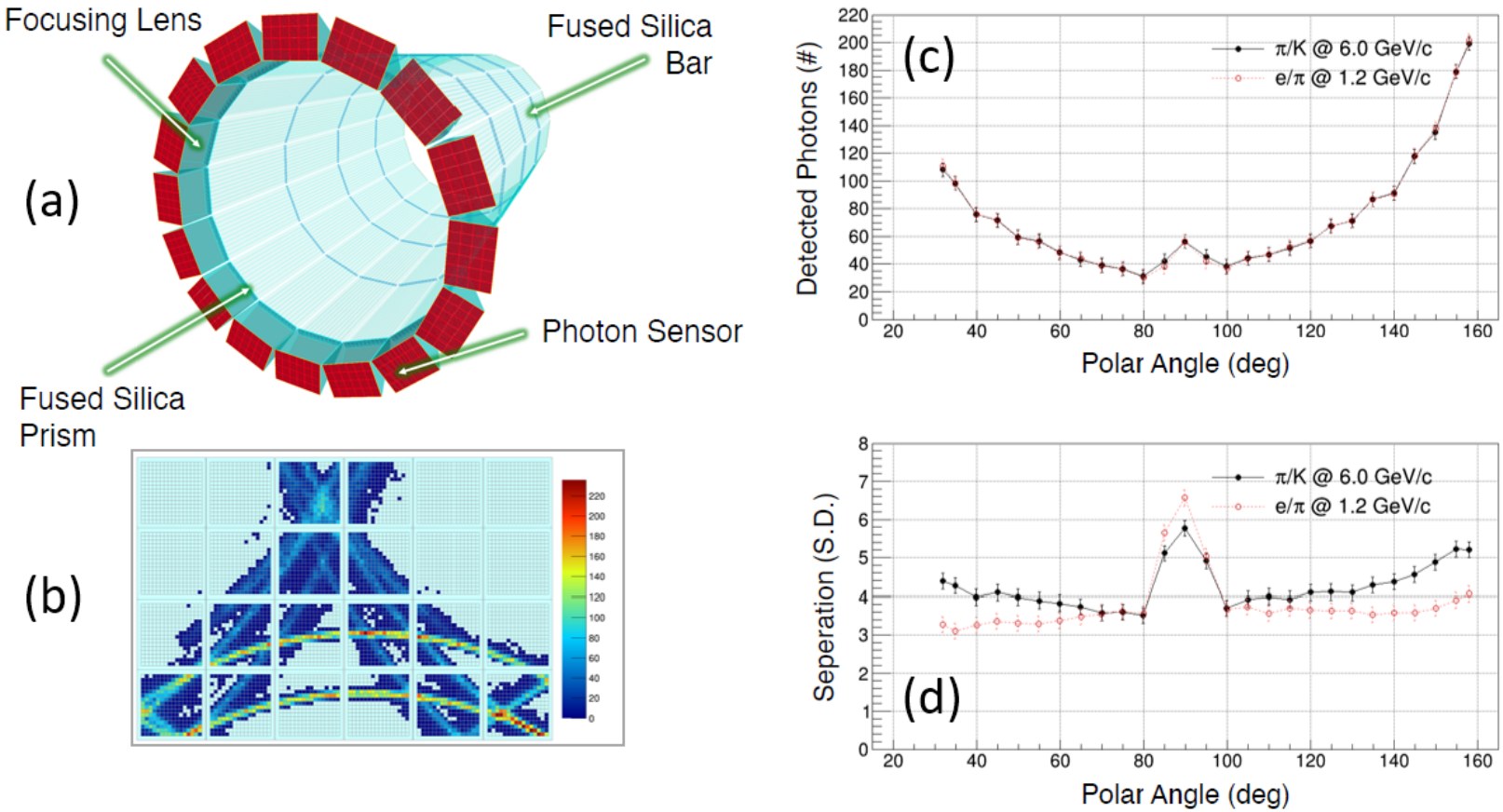

Figure 2.9: a) Configuration of the DIRC. b) Superposition of the distribution of photon hits from 6 GeV/c identical pions. c) Number of detected photoelectrons as a function of polar angle. d) Separation power at the maximum momentum requirement stated in the Yellow Report. Results from a stand-alone GEANT4 simulation.

- high performance DIRC (detection of internally reflected cherenkov light)

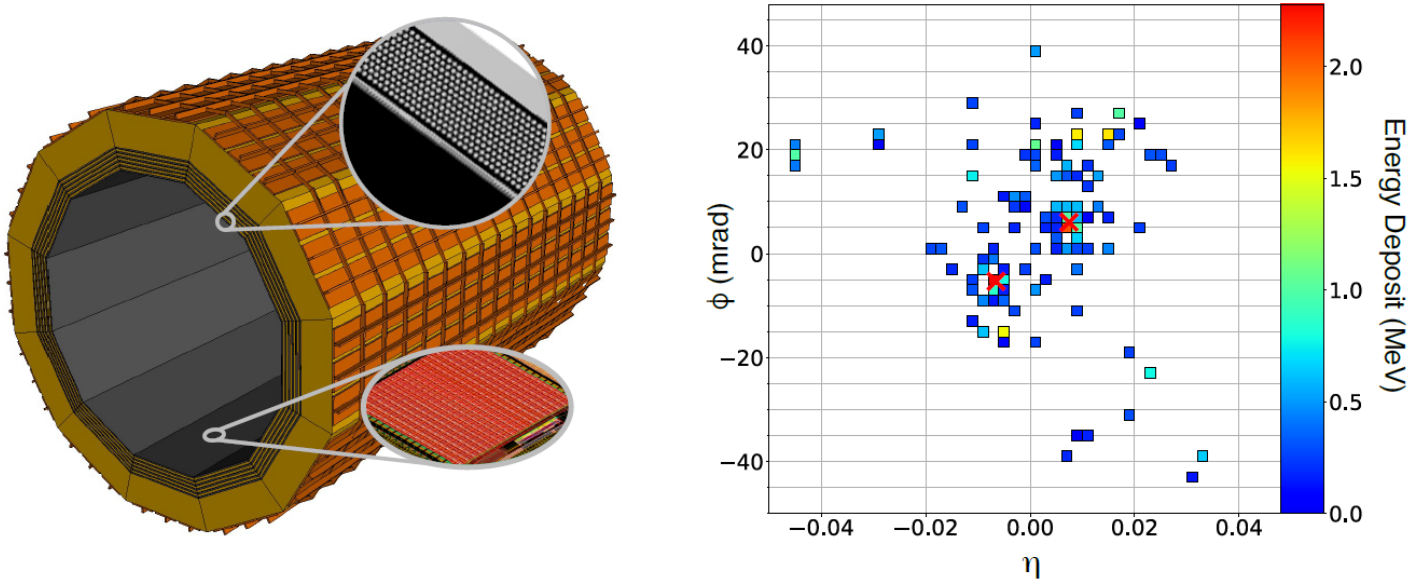

Figure 2.6: Left: The barrel electromagnetic calorimeter as included in detector simulations. The inner radius of the barrel is 103 cm. The first (closest to the beam) 6 layers are imaging layers. The insets show the structure of the Si imaging layers (bottom) and the 1.59 cm thick Pb/SciFi (top). The imaging layers are followed by a thicker Pb/ScFi section, for a total thickness (not including the support structure) of 40 cm. Right: Energy deposited in pixels in the imaging calorimeter demonstrating clean seperation of the two clusters for a 15 GeV π^0. The red crosses mark the reconstructed clusters centers (FullSim).

- Hybrid Pb/SciFi design and imaging with monolithic silicon sensors (AstroPix)
  - 6 layers of silicon sensors
  - 5 layers of Pb/SciFi (1.59 cm) + thick layer of Pb/SciFi
- Outer layer causes 70% of neutrons to shower, which helps identify neutral hadrons
- Hybrid+imaging calorimeter allows use of machine learning techniques for patter recognition of showers in 3D
  - Enables muon identification

Barrel E-M Calorimeter performance

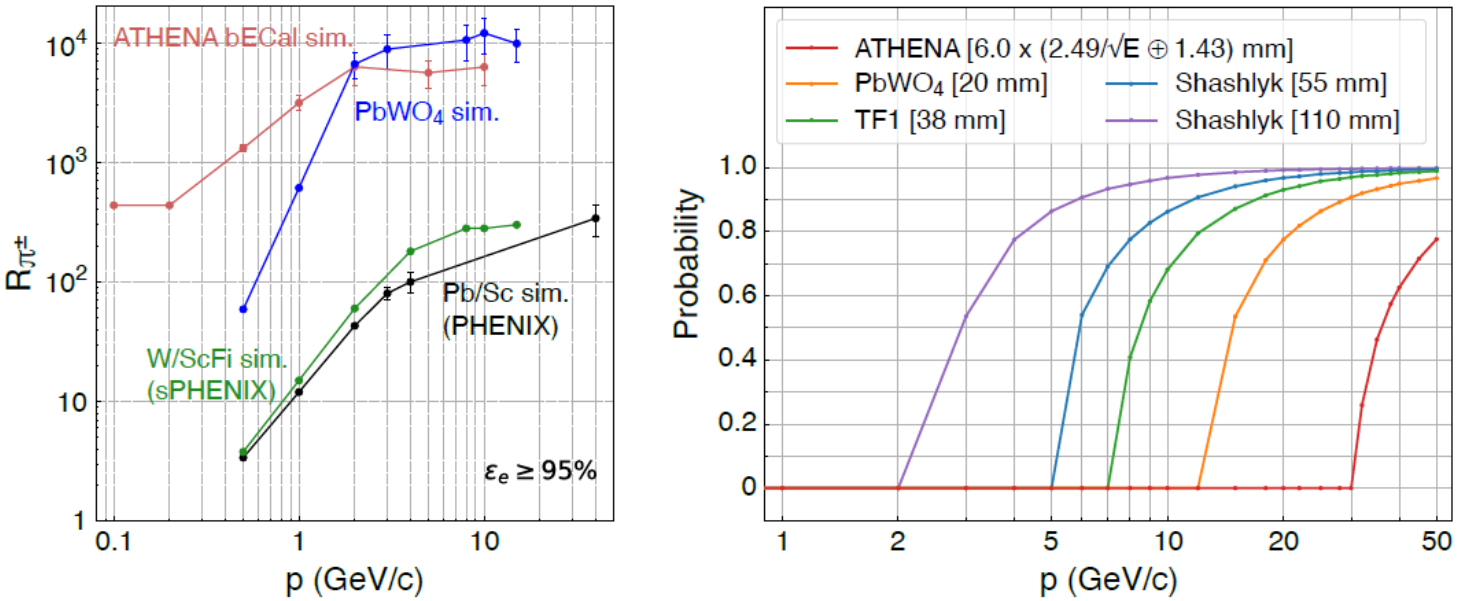

Figure 2.7: Left: The pion rejection power of ATHENA bECal (red solid line) compared with other technologies listed in the EIC Yellow Report. The rejection power of the ATHENA bECal is obtained from the analysis described in the Supplemental Material utilizing the E/p method and pattern matching, while the other rejection powers are determined from the E/p method [3] only. All the curves, including simulations and data, are obtained for the standalone calorimeter, *i.e.*, no other materials are placed in front of the calorimeter and no magnetic field is involved. The effects of material and the magnetic field are discussed further in the supplemental material. Right: The merging probability of the two γs from π^0 decay in the barrel region at r = 1.03 m. For ATHENA bECal, 6σ of its spatial resolution ($2.4/\sqrt{E} \oplus 1.3$ mm) is used to estimate the merging probability, since its pixel size (0.5 mm) is much smaller than the cluster profile. For the other technologies, the cell size is used to estimate the probability [3].

Table 2.3: Expected bECal detector performance.

Energy Resolution	$5.5\%/\sqrt{E} \oplus 1\%^{a}$
e/π separation	$>$ 99.8% pion rejection with 95% electron efficiency at $p \geq 0.1$ GeV/c^{b}.
E^{γ}_{min}	< 100 MeV^{c}
Spatial Resolution	Cluster position resolution for 5 GeV photons at normal incident angle is below $\sigma = 2$ mm (at the surface of the stave $r = 103$ cm) or 0.12°. For comparison, the minimal opening angle of photons from $\pi^0 \to \gamma\gamma$ at 15 GeV is $\sim 1.05°$ (about 19 mm – 37 pixels – of separation at $r = 103$ cm).

[a] Based on the photon simulations with $-0.5 < \eta < 0.5$ and $0 < \phi < 2\pi$. The constant term does not include calibration effects.
[b] Based on simulation for a standalone bECal, see Fig. 2.7 for detailed results.
[c] Based on simulations, 100 MeV photons leave an energy deposit of $\sim$ 15 MeV in SciFi layers and of $\sim$ 1 MeV in the imaging layers. This simulation includes digitization with electronics noise and a noise suppression cut.

Negative E-M calorimeter (nECal)

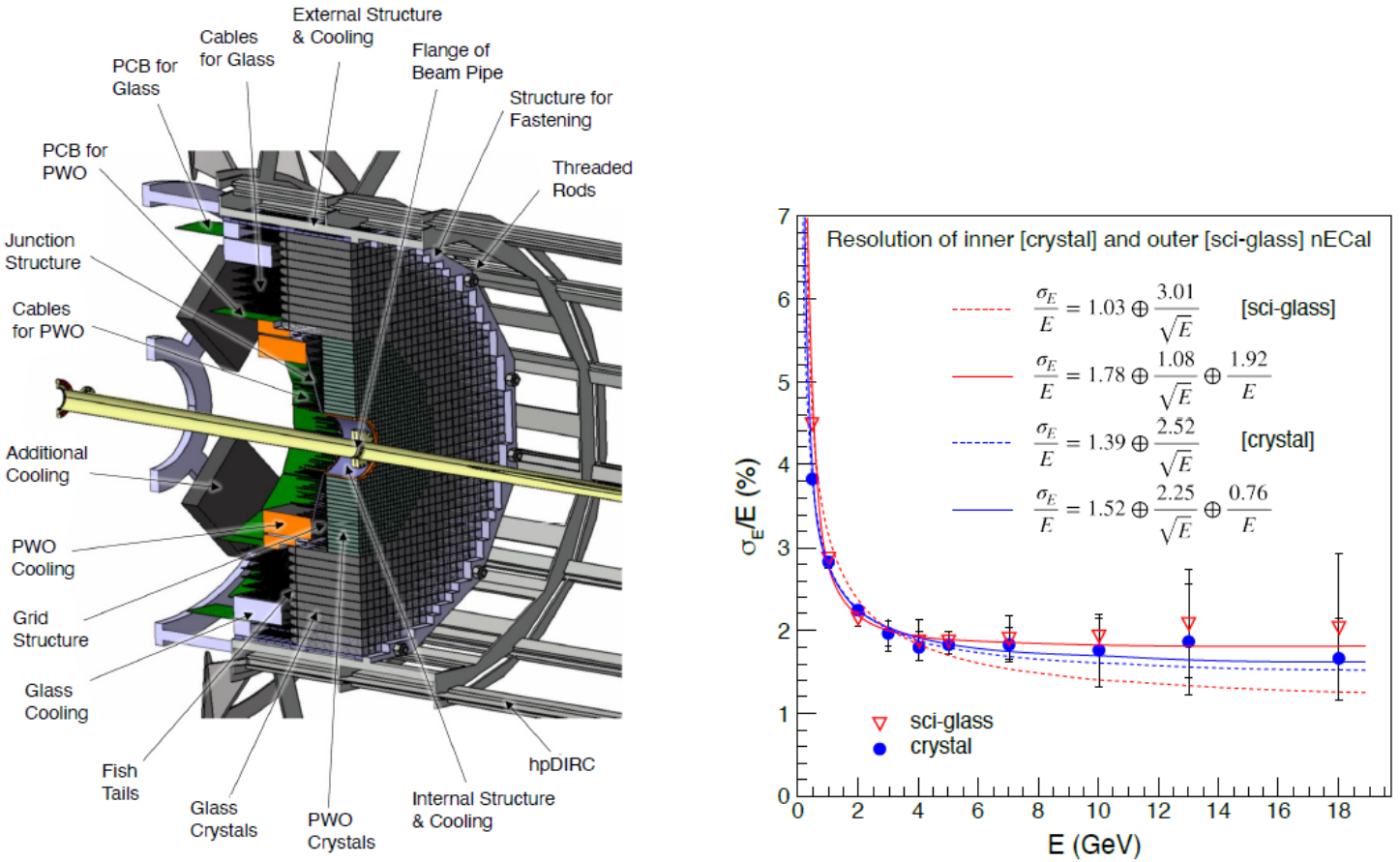

Figure 2.5: Left: The mechanical design of hybrid crystal/glass calorimeter nECal. Right: Expected nECal performance for the stand alone calorimeter, the energy resolution curves for inner $PbWO_4$ ($\sim 22\ X_0$) and outer SciGlass ($\sim 20\ X_0$) regions (FullSim).

- Located in the negative *e*-going (backward) direction
- Inner part: PbWo4 crystals
- Outer part: SciGlass

dRICH (forward)

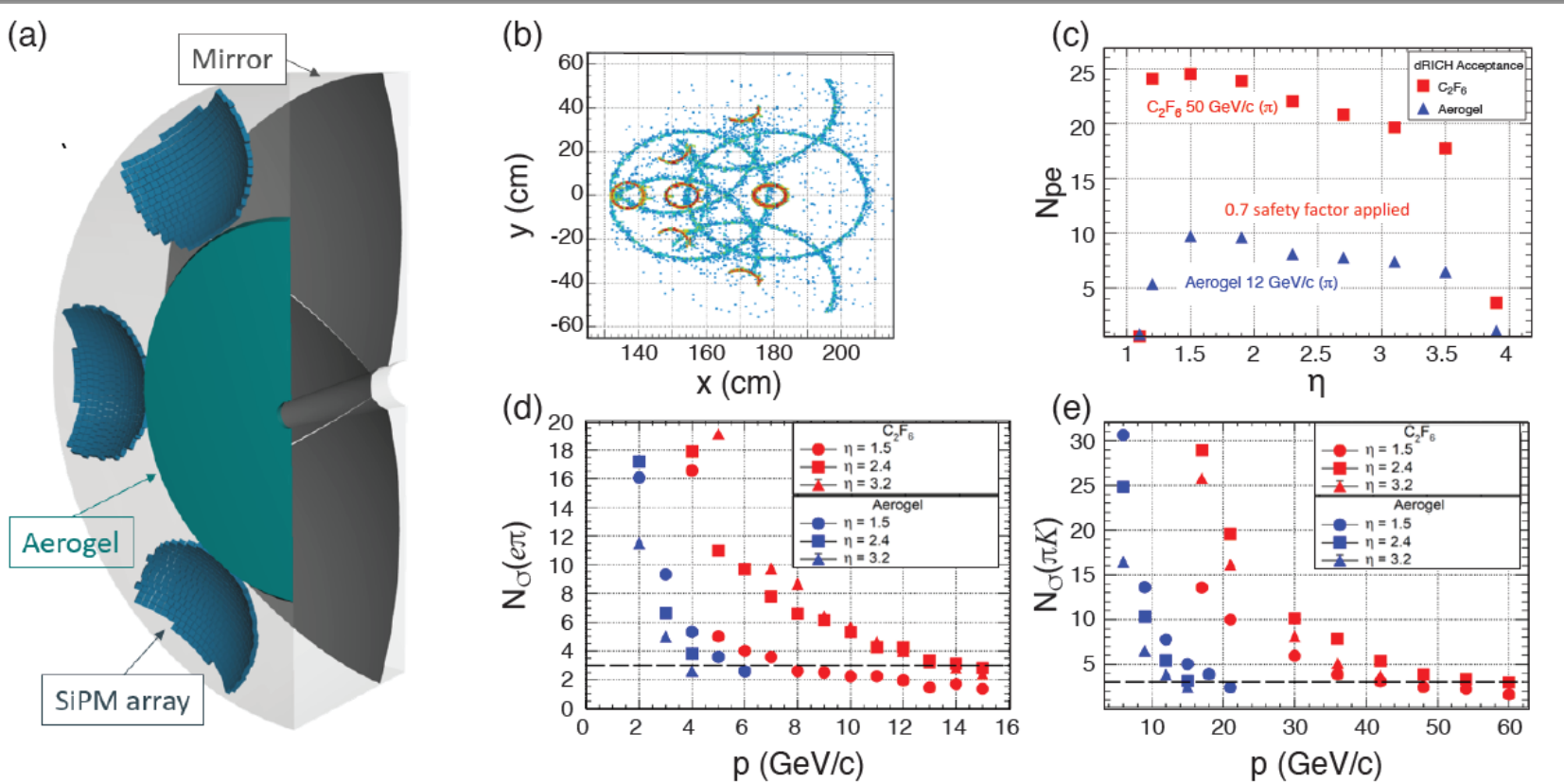

Figure 2.8: Panel a) shows the layout of the dRICH radiators, mirror, and SiPM focal planes. Panel b) shows the superposition of hits from 1000 events with identical primary particles. This effectively captures ring shape (aerogel-large, gas-small), Rayleigh scattering, optical aberration, multiple scattering, tracking resolution, chromaticity, and signal-to-noise effects in one image. Panel c) shows the number of photoelectrons per single ring vs η, and thereby illustrates the acceptance range. Panels d) and e) demonstrate the PID separation for $e\pi$ and πK. The performance meets the Yellow Report specification. Aerogel performance is indicated in blue and C_2F_6 in red (FullSim).

- Dual-radiator RICH at forward rapidity (p-going)
- Good e/π separation

Muon detection - barrel

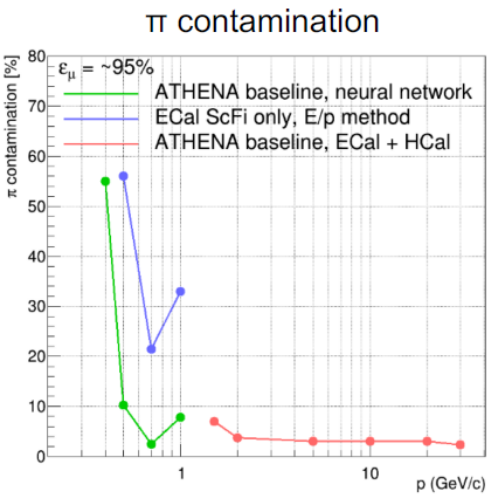

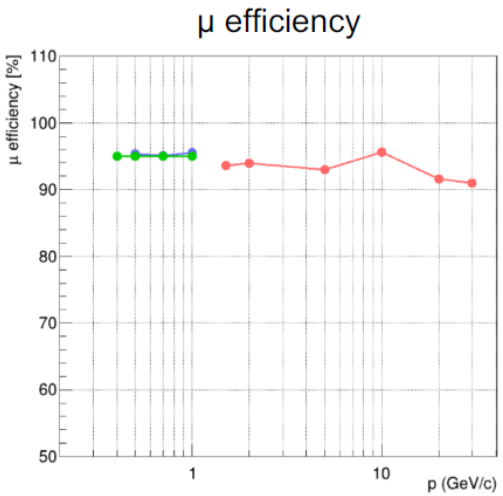

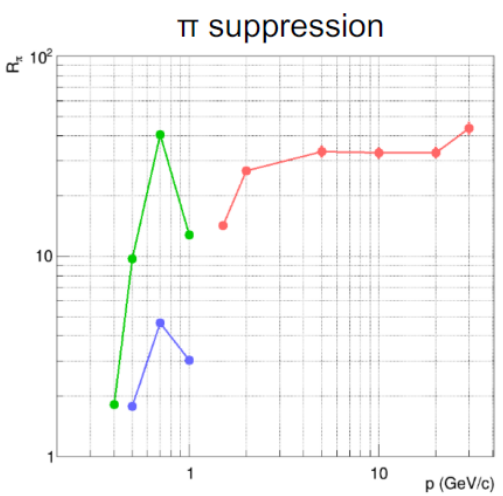

- Information from Barrel E-M and hadronic calorimeters allows to separate μ/π
- Muons with $p > 1.5\,\mathrm{GeV/c}$ reach BHCal
- For $p < 1.5\,\mathrm{GeV/c}$ they curl inside BECal
- Better performance if other PID detectors included

Muon detection - barrel

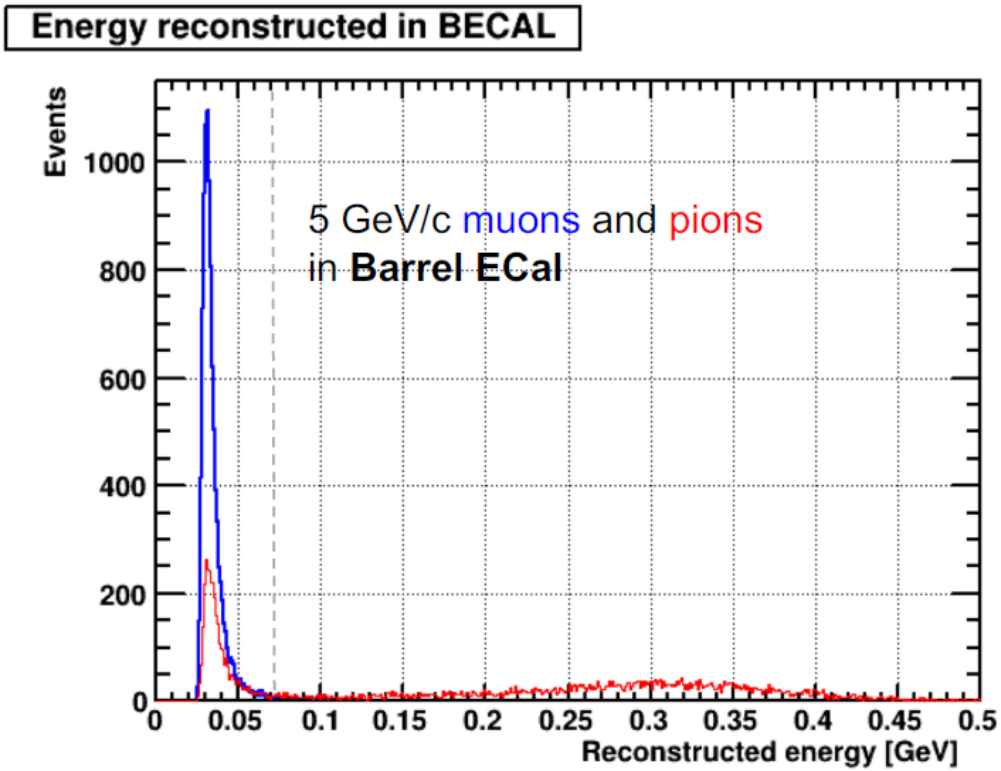

- μ leave MIP signal in BECal
- μ selection:
  - MIP signal in BECal (95% efficiency)
  - hits in each BHCal layers

Muon detection - barrel

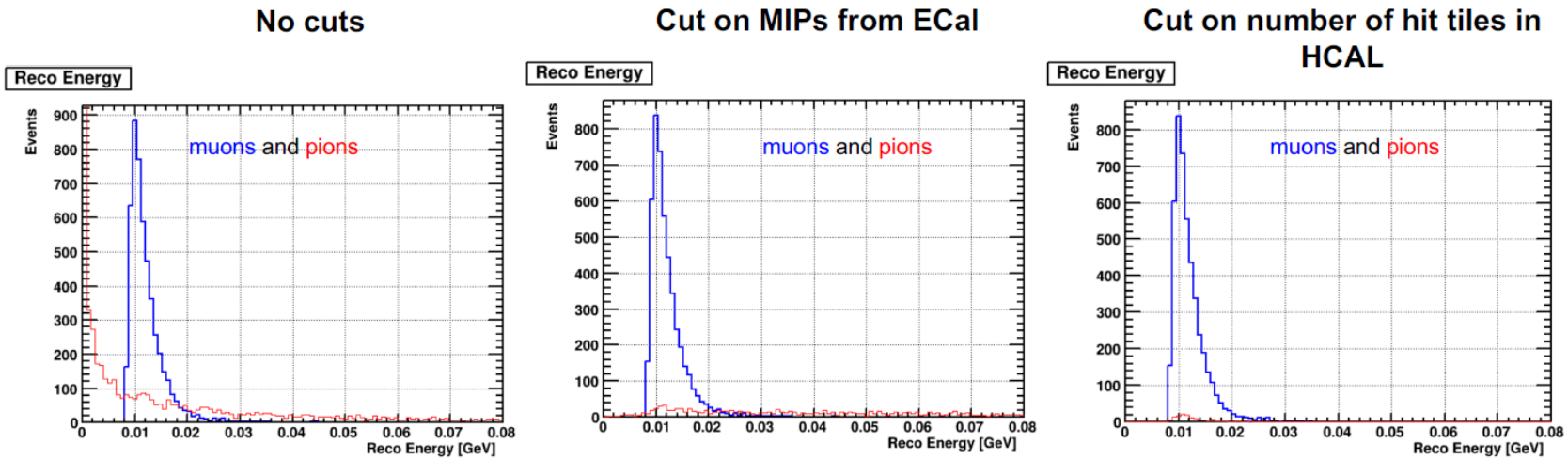

- μ leave MIP signal in BECal
- μ selection:
  - MIP signal in BECal (95% efficiency)
  - hits in each BHCal layers

Example of **muons** and **pions** at **p = 0.5 GeV/c** at η = (-1,1)
Efficiency: 98.9% ⟶ Rejection Power: 6.6
Efficiency: 95% ⟶ Rejection Power: 9.7

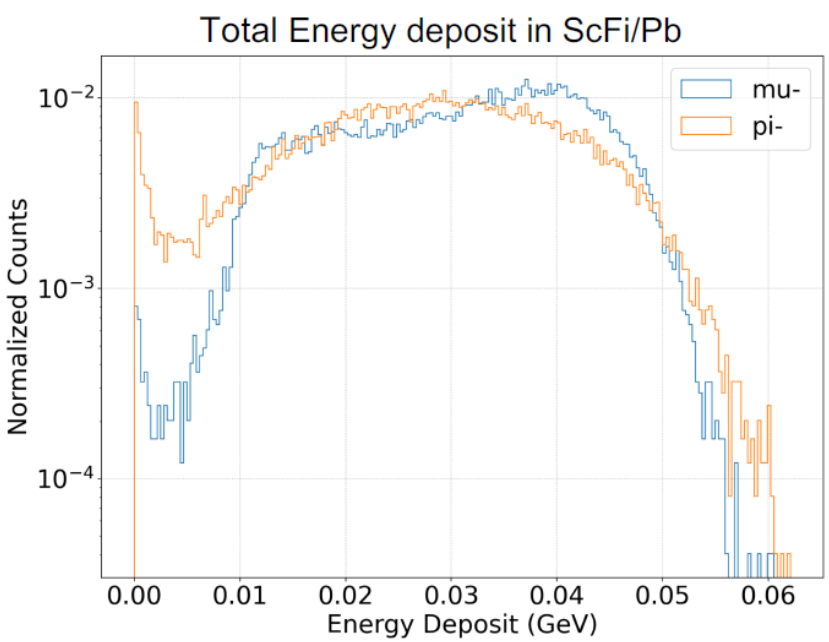

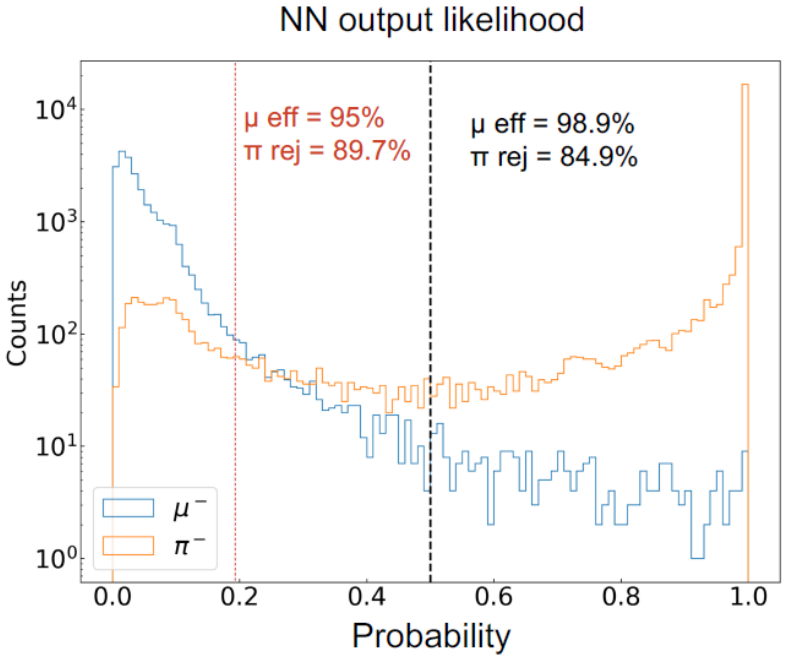

Comparing the two plots demonstrates the power of including the imaging layers:
→ they enhance μ/π separation at low momenta

- Muon identification using information from imaging layers and Pb/SciFi of BECal and machine learning
  - 4 parameters for each hit: η, ϕ, E, R
  - 3 layers convolutional neural network and 3 layers perceptron
  - 95% efficiency

Muon detection - forward (hadron endcap)

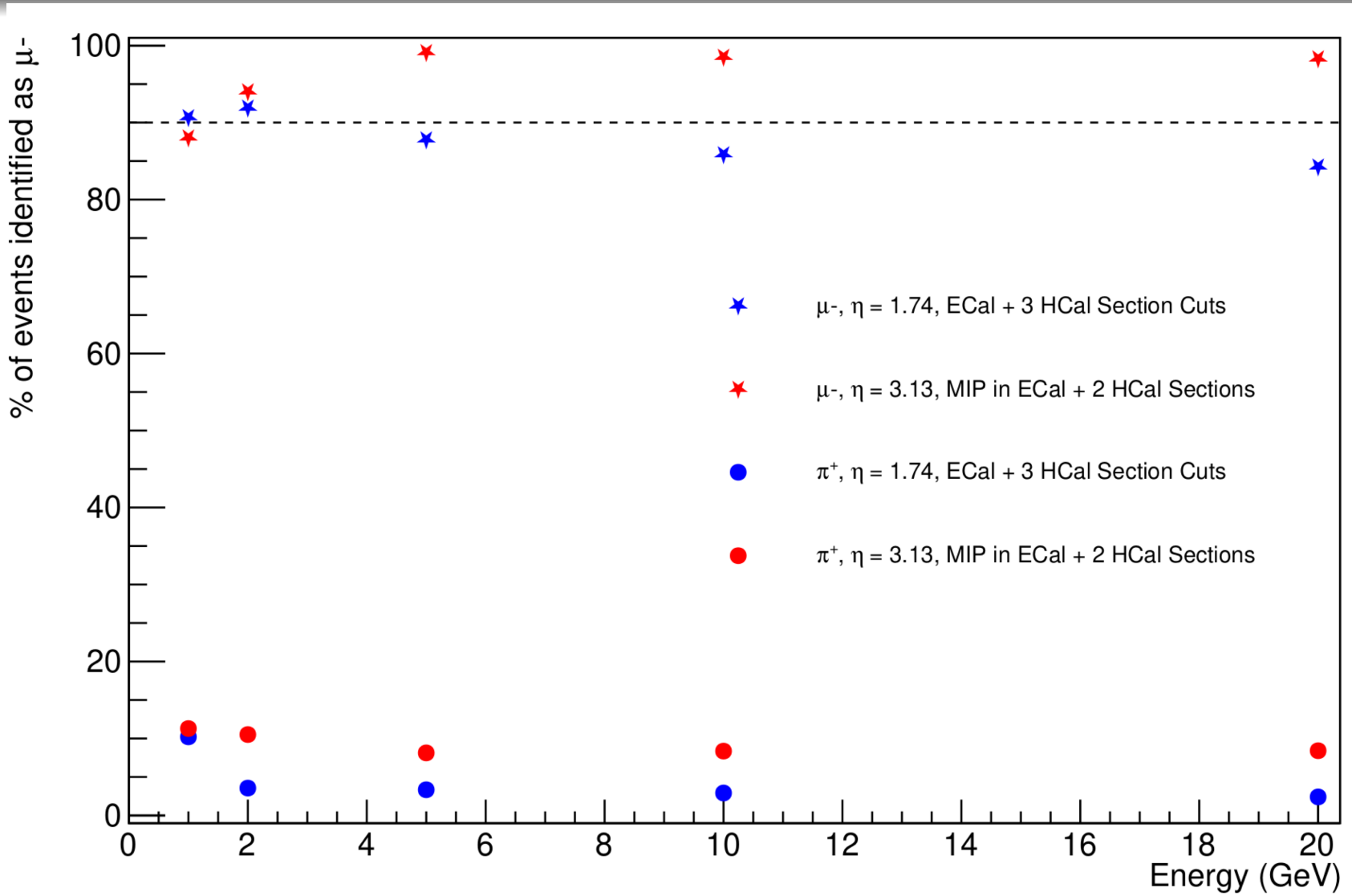

- Muon selection possible with pECal and pHCal information
  - MIP-like signal in pECal
  - Number of hits along the tracks consistent with no shower
- 90% efficiency, only few % pion contamination

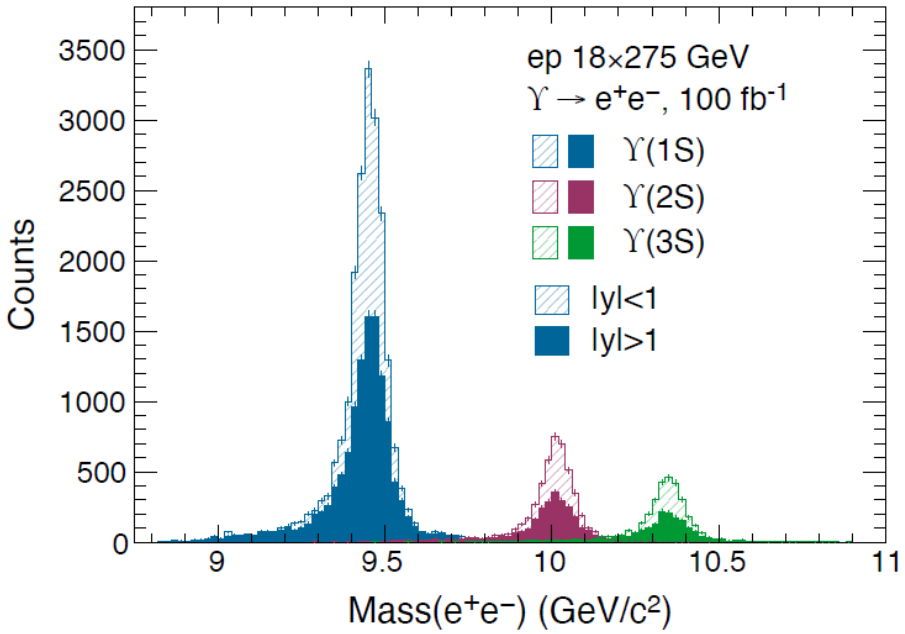

Figure 3.5: The simulated M_{ee} mass spectrum for exclusive production of the three Υ states in 18 $\times$ 275 GeV e+p with 100 fb^{-1} of integrated luminosity, using the cross sections from eSTARlight [58]. Spectra are shown for Υ-production at mid-rapidity ($|y| < 1$) and away from mid-rapidity ($|y| > 1$) (FullSim).

- Upsilon states well separated in the dielectron channel
- Low bremsstrahlung tails thanks to low-mass trackers and beampipe

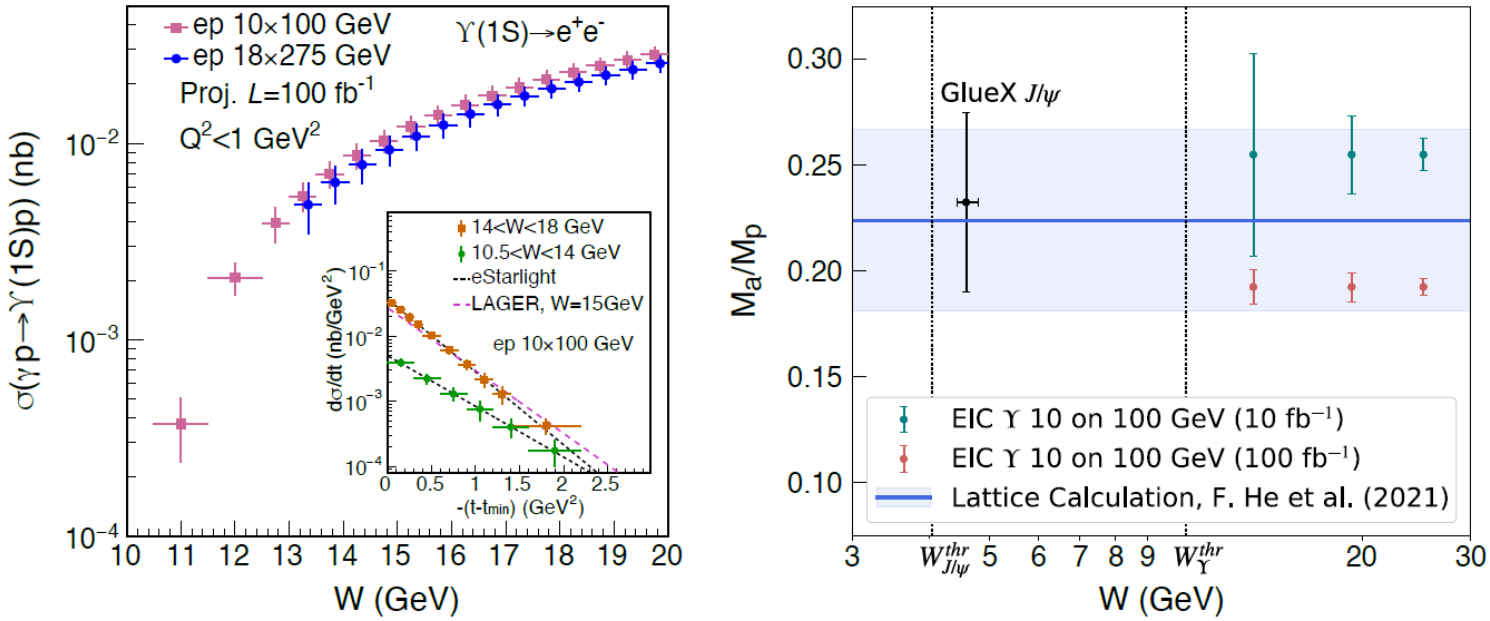

Figure 3.19: Left: The projected uncertainty of total and differential (insert panel) cross section of $\Upsilon(1S)$ near threshold for photo-production and electro-production ($Q^2 < 1$ GeV^2) in e+p collisions via the di-electron decay channel. Two model predictions [58, 101] of the near threshold differential $d\sigma/dt$ are also shown (FullSim). Right: The trace anomaly contribution to the proton mass in Ji's decomposition according to [104, 105] and references therein. Green and red points correspond to 10 fb^{-1} and 100 fb^{-1} integrated luminosity, respectively, and are offset from each other. The band is the result of a recent lattice QCD calculation [106] (FullSim).

- Needs measurement of electron and/or proton momentum
- Projections both for 10 fb^{-1} and 100 fb^{-1}

Summary

- Good performance for Upsilon states separation
- Muon detection possible with ECal+HCal

BACKUP

Magnet

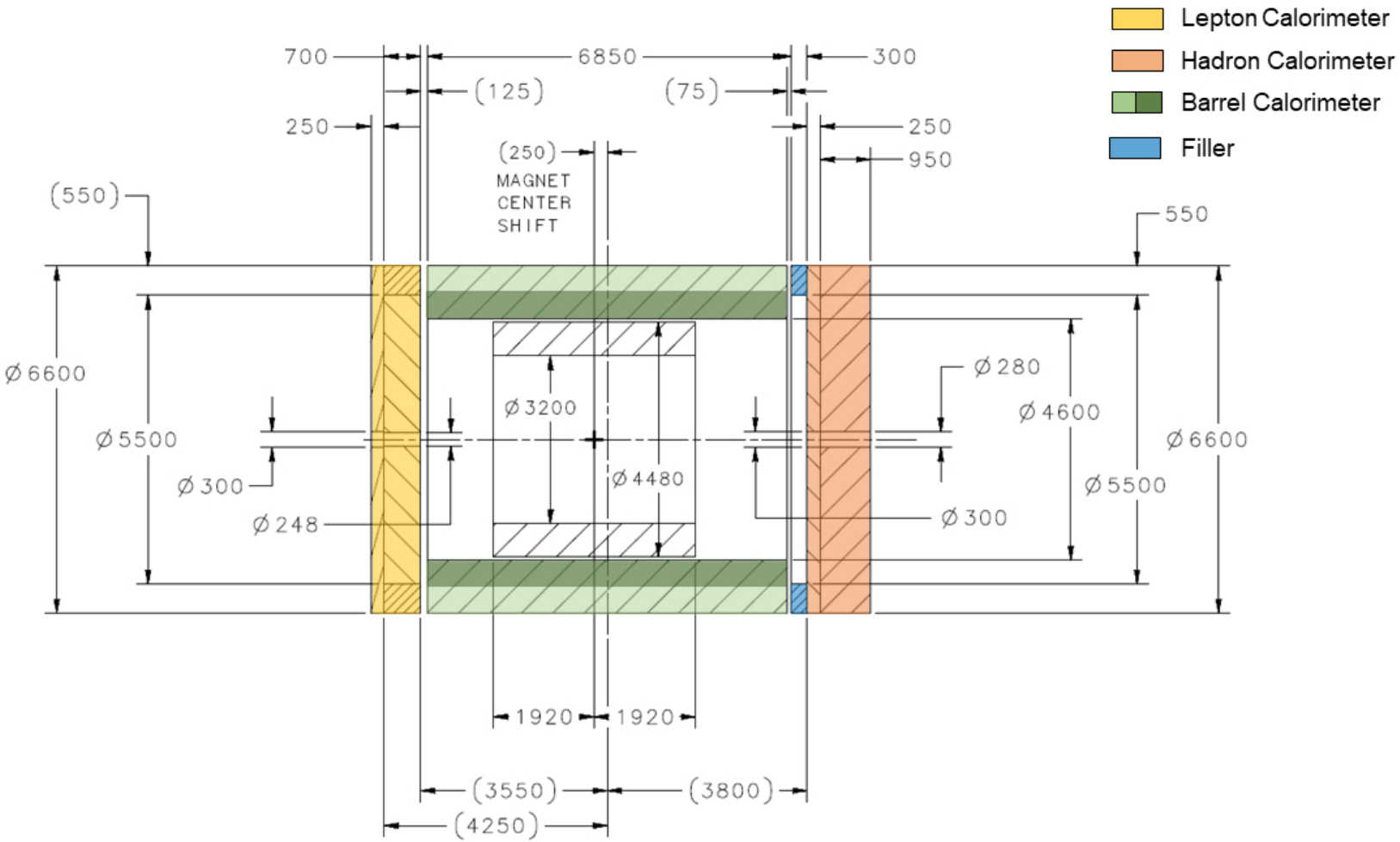

- superconducting magnet
- 3T solenoidal magnetic field
- lower settings possible

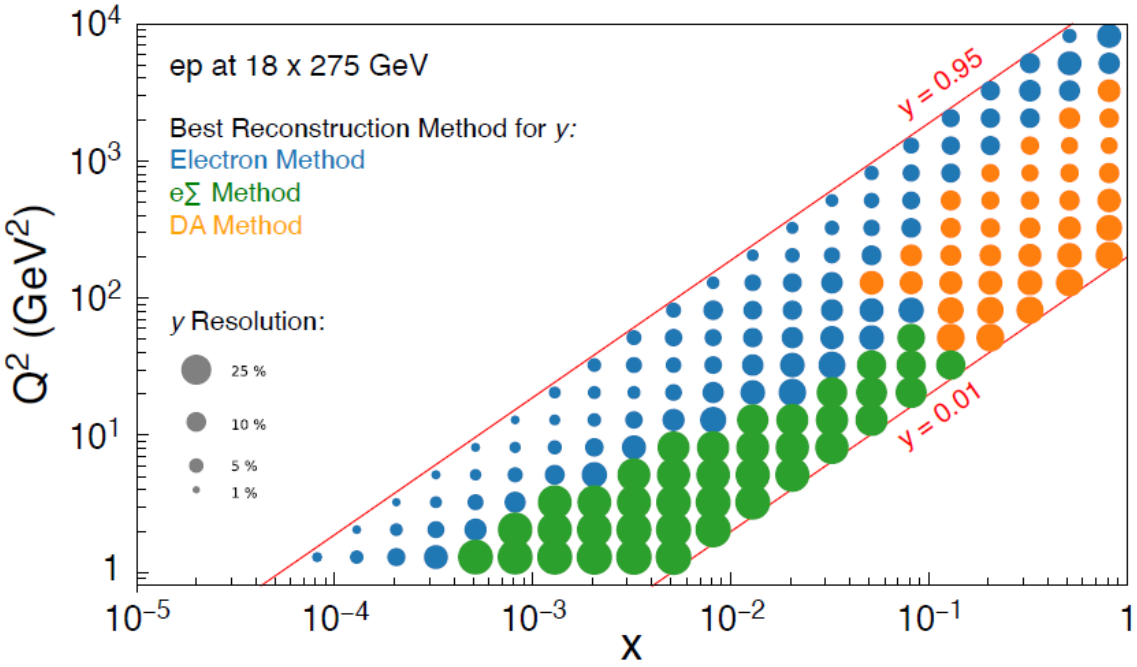

Figure 3.1: Variation of the estimated ATHENA resolution on the kinematic variable, y, with x and Q^2, for the example case of 18 GeV electrons colliding with 275 GeV protons. At each point in the kinematic plane, the best performing reconstruction method is chosen and indicated by the color of the corresponding marker, while the size of the marker indicates the magnitude of the resolution obtained (FullSim).

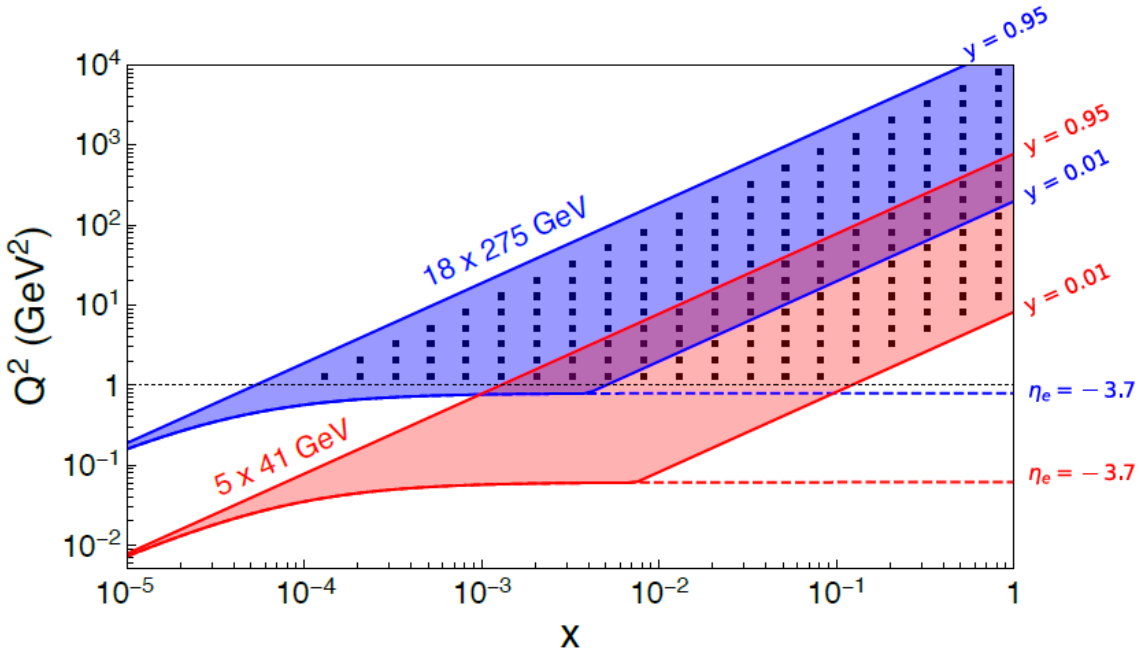

Figure 3.2: Kinematic coverage of simulated ATHENA data for EIC running at the largest and smallest center-of-mass energies. The positions in the kinematic plane of simulated measurements in the deep-inelastic region with selection requirements: $Q^2 > 1$ GeV^2 and $0.01 < y < 0.95$ (FullSim).

BECal performance

Baseline ATHENA ECal

pfRICH
- n=1.02
- $\pi_{threshold}$=0.69 GeV/c
- Cuts set at 90%, 95%, 98% electron efficiency
- Background hits not included.

TOF
- $\sigma_T = 30ps \oplus 20ps$
- $\sigma_T = 36\ ps$
- Analytical Response

DIRC
- n=1.473
- $\pi_{threshold}$=0.13 GeV/c
- Tabulated from FullSim

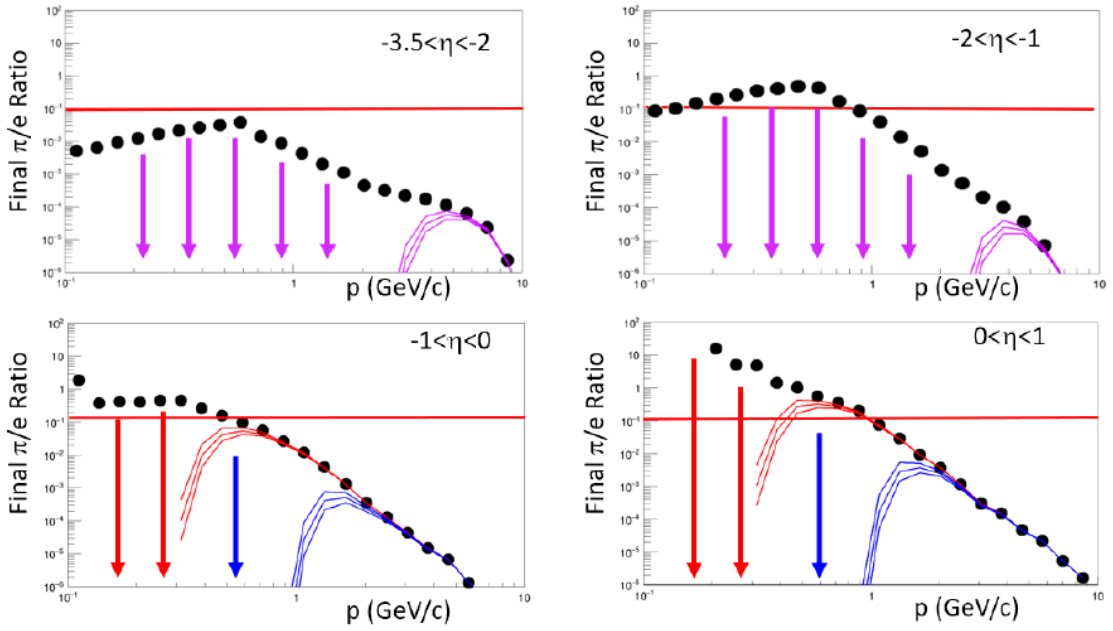

FastSim results; below 10^{-6} indicated by downward arrows